Office Note 463

Southeast Pacific low-cloud simulation in the NCEP GFS: role of vertical mixing and shallow convection

Shrinivas Moorthi,
Environment Modeling Center

Ruiyu Sun,
UCAR/Environment Modeling Center

Heng Xiao
Robert. C. Mechoso
Department of Atmospheric Science and Oceanic Sciences,
7127 Math Sciences Building, 405 Hilgard Avenue,
Los Angeles, California 90095-1565

Corresponding author address: 5200 Auth Rd., Camp Springs, MD, 20746

E-mail: shrinivas.moorthi@noaa.gov

1

ABSTRACT

Two simple modifications are made in the physics of the NCEP Global Forecast System (GFS) model to alleviate an important systematic error: the lack of stratocumulus in the southeast Pacific region. A preliminary step consists of estimating the location of a low-level inversion at each grid point. The modifications are based on (a) elimination of background vertical diffusion above the low-level inversion and (b) incorporation of a tunable parameter based on the cloud-top entrainment instability (CTEI) criterion, according to which shallow convection does not destroy the inversion when it is strong. A control simulation and three additional experiments are performed to examine the individual effect of each modification and the combined effect of the two modifications on the generation of the stratocumulus clouds. It is found that both modifications result in enhanced cloudiness in the Southeast Pacific (SEP) region, although cloudiness is still low in reference to the ISCCP climatology. If the two modifications are applied together, however, the total cloudiness produced in the southeast Pacific has realistic values. This nonlinearity arises as both modifications reinforce each other in reducing the leakage of moisture across the inversion. Less mixing traps more moisture at low levels below the inversion and results in more condensation. In generating clouds, the large-scale condensation process was the main contributor. The convective parameterization also provided a positive, but smaller contribution. Although the amount of total cloudiness obtained with both modifications has the correct magnitude, the relative contributions of low, middle, and high layers may differ from the observed. Our experiments demonstrate that it is possible to simulate realistic marine boundary clouds in large-scale models with relatively simple and physically based changes in the model parameterizations.

2

1. Introduction

The climatology of the tropical and subtropical Pacific Ocean south of the Equator is characterized by large east-west gradients in sea surface temperature (SST), with values increasing from ~ 20°C along the South American coast to ~29°C in the Western warm pool. Going west up the SST gradient, the dominant cloud type changes from stratocumulus with high coverage near the coast, to shallow cumulus with much lower coverage over the central Pacific. This evolution of cloud regimes occurs in the descending branch of the atmospheric Hadley-Walker circulation with trade winds along the surface, and a trade wind inversion in the lower troposphere that elevates and weakens along the direction of the SST gradients. In this broad sense, the Southeast Pacific (SEP) climate is a tightly coupled system, in which poorly understood interactions develop among clouds, marine boundary layer (MBL) processes, upper ocean dynamics and thermodynamics, coastal currents and upwelling, large-scale subsidence, and regional diurnal circulations, and aerosol effects. Interactions among the South American continent and the atmosphere-ocean system in the SEP are extremely important components of both the regional and global climate. The great height and length of the Andes Cordillera forms a sharp barrier to the zonal flow, resulting in a coastal jet of strong, low-level southerly winds parallel to the west coast of South America (Garreaud and Muñoz, 2004). This, in turn, drives intense coastal oceanic upwelling, bringing cold, deep, and nutrient/biota rich waters to the surface. As a result, the SST is colder along the Chilean and Peruvian coasts than at any comparable latitude elsewhere in the world. The cold surface, in combination with subsiding warm, dry air aloft, is ideal for the formation of marine stratocumulus clouds, which extend almost 2,000 km west from the Peruvian Coast. It supports the world's largest and most persistent subtropical stratocumulus cloud deck (Klein and Hartmann 1993; Kollias et al. 2004). The existence of this stratus cloud deck has a major impact upon the earth's radiation budget (Ma et al. 1996; Gordon et al. 2000). Difficulties in the prediction of these marine boundary layer clouds in climate models significantly contribute to the tropical cloud feedback uncertainties (Bony and Dufresre 2005). Most atmosphere-ocean coupled general circulation models (CGCMs) lack the ability to produce a realistic cloud deck in the eastern tropical oceans (Mechoso

et al. 1995; Ma et al. 1996, Hannay et al. 2009), including the current and earlier operational versions of the National Center for Environmental Prediction (NCEP)'s Global Forecast System (GFS). Underprediction of stratus results in overestimation of heat flux into the ocean and may be the primary reason why the ocean-atmosphere coupled models show positive SST biases of several degrees off the coast of Peru (Mechoso et al. 1995; Wang et al. 2005; de Szoeke et al. 2006).

These model difficulties are most clear in the 2003 version of the operational GFS, which has been used since 2003 as the atmospheric component of the Climate Forecast System (CFS) to produce operational climate forecasts at NCEP (Saha et al. 2005). The CFS obtains ENSO-like interannual variation in the tropical Pacific with reasonable temporal and spatial patterns (Wang et al. 2005). However, the CFS produces large errors in the simulated mean SST, especially along the South American coast and in the Pacific "equatorial cold tongue" region. These errors are primarily attributable to the lack of sufficient stratocumulus in the operational CFS and results in an incorrect simulation of the surface radiation budget.

At NCEP, several approaches are being followed to improve the representation of cloudiness in the SEP and over the subtropical oceans in general. The present paper reports on a series of studies aimed at improving the stratocumulus and coupled climatology of the operational GFS/CFS. We search for simple yet physically based revisions of the representation of inversion temperature/moisture jumps in the atmosphere and their controls on the depth of shallow convection. The revisions made and used in the CFS reanalysis (CFSR) improve low cloud cover over the eastern subtropical oceans.

The text is organized as follows. We start in section 2 by providing a brief description of the operational NCEP/GFS. Section 3 presents the changes made to the GFS physics to address the stratus issue. Section 4 describes the experiments. Sections 5, 6 and 7 show experimental results. Section 8 summarizes the work presented and conclusions reached.

2.   **Brief GFS model description**

The current GFS uses a spectral triangular truncation of 382 waves (T382) in the horizontal (equivalent to nearly a 35 km Gaussian grid), and a hybrid sigma-pressure

finite differencing system (Sela 2009) in the vertical with 64 layers. The model top layer is at ~ 0.2 hPa.

This GFS version has undergone significant improvements from the version of the NCEP model used for the NCEP/NCAR Reanalysis (Kalnay et al. 1996; Kistler et al. 2001). These include upgrades in the parameterization of solar radiation transfer (Hou et al., 1996 and Hou et al. 2002), boundary layer vertical diffusion (Hong and Pan 1996), Simplified Arakawa-Schubert (SAS) cumulus convection (Pan and Wu 1995; Hong and Pan 1998), and gravity wave drag (Kim and Arakawa 1995). In addition, cloud condensate is a prognostic variable (Moorthi et al. 2001) with a simple cloud microphysics parameterization (Zhao and Carr 1997; Sundqvist et al. 1989). Both large-scale condensation and detrainment of cloud water from cumulus convection provide sources of cloud condensate.

The fractional cloud cover used in the radiation calculation is diagnostically determined from the predicted cloud condensate based on the approach of Xu and Randall (1996). The contribution of convection to cloud cover is through detrained condensate only; there is no explicit "convective cloud cover". The operational GFS also uses the Rapid Radiative Transfer Model (RRTM) longwave parameterization from Atmospheric and Environmental Research Inc. (AER, Mlawer et al. 1997) with maximum/random cloud overlap and a modified version of the National Aeronautics and Space Administration (NASA) Goddard Space Flight Center (GSFC) shortwave radiation (Hou et al. 2002, Chou et al. 1998) with random overlap. The latter scheme is known to overestimate shortwave radiation under cloudy conditions.

Ozone is a prognostic variable with a simple parameterization for ozone production and destruction. The model also incorporates a four-layer NCEP-Oregon State University-Air Force-Hydrological Research Lab (Noah) land-surface model (Ek et al., 2003). In addition to gravity-wave drag, a parameterization of mountain blocking (Jordan, 2004) is included, following the subgrid-scale orographic drag parameterization by Lott and Miller (1997).

The shallow convection parameterization follows Tiedtke (1983), and is applied wherever the deep convection parameterization is not active. In this scheme, the highest positively buoyant level below $0.7 * P_s$ (where P_s is surface pressure) for a test parcel

5

from the second model layer is defined as the shallow convection cloud top. The cloud base is the lifting condensation level (LCL) for the same test parcel. Enhanced vertical eddy diffusion is applied on temperature and specific humidity within this cloud layer; the diffusion coefficients are prescribed with a maximum value of 5 m^2s^{-1} near the cloud center and approaching zero near the edges.

3. Modifications of the GFS

The parameterization of shallow convection plays a vital role in the formation and/or destruction of marine stratocumulus. Wang et al. (2004) found, in their regional model simulation of boundary layer clouds, that turning off the shallow convection parameterization dramatically increased shallow clouds. de Szoeke et al. (2006) examined the effect of shallow convection on the eastern Pacific climate using a regional ocean-atmosphere model. They found that shallow convection acts to destroy stratus clouds and with no shallow convection the stratiform cloud fraction increases resulting in an excessive SST cooling.

As a first step we introduce the consideration of an inversion into the shallow convection scheme, which hitherto was ignored in the GFS. Since shallow clouds are allowed in the simulations to extend from the LCL up to 0.7 P_s, they can actually extend across the inversion layer irrespective of its strength. Very strong inversions are expected to limit the vertical extent of shallow cloud. Instead, shallow convection leads to an erroneous weakening of the inversion in all cases. This process also results in excessive drying and warming of the layers below the inversion, where the cloud amount is severely limited. In addition, it facilitates leakage of moisture across the inversion into the free atmosphere above, which in turn inhibits formation of low-level clouds.

To overcome these difficulties, we start by introducing a definition of low-level inversion as the region comprised by model layers below 0.65P_s in which dT/dP satisfies the following requirements: (1) is less than 0.0001 K/Pa, where T and P are temperature and pressure respectively, and (2) changes sign at one or two layers below. Next, we require the mixing associated with shallow convection to be confined below the inversion, thus limiting the effect of the former on the latter. For this we must develop a criterion that represents both the existence of shallow convection and the inversion

strength. Such a criterion can be based on the cloud-top entrainment-instability (CTEI) concept, which has been used in GCMs for several decades in an attempt to represent the large-scale control on PBL clouds (Deardorff 1980; Randall 1980; Suarez et al. 1983). In its original formulation, CTEI predicts runaway entrainment and rapid destruction of stratocumulus when the following condition holds,

$$\kappa = c_p \Delta\theta_e / L\Delta q_t > \kappa_0, \tag{1}$$

where c_p is the specific heat of dry air under constant pressure, L is the latent heat of water vaporization, $\Delta\theta_e$ is the jump of equivalent potential temperature, and Δq_t is the jump of total water mixing ratio across the inversion. According to Randall (1980) and Deardorff (1980) an appropriate value to be used in the right hand side of (1) is $\kappa_0 = 0.23$. As pointed out by many authors (e.g., Kuo and Schubert 1988; Moeng 2000; Stevens et al. 2005; Siems et al. 1990), Equation (1) only gives the possibility of buoyancy reversals when entrained air is mixed with cloudy air and cooled by cloud water evaporation. Clouds may still remain and entrainment may not change abruptly because (1) the fraction of denser mixtures generated for κ slightly larger than κ_0 may be too small to cause instability, and (2) these denser mixtures may not directly enhance the intensity of entraining eddies at cloud top. Other possible responses to entrainment drying, like enhanced surface moisture flux, could even refill and deepen the cloud layer. Despite these caveats, simulations with Large Eddy Simulation Models (LES) in cases with both well-mixed and decoupled PBL setups have shown significant anti-correlation between cloud fraction and κ (Moeng 2000; Lock 2009). For κ large enough (0.6~0.7), cloud fraction around 0.1~0.2 are always found. In this study we choose $\kappa > \kappa_0 = 0.7$ following MacVean and Mason (1990). In view of these considerations, we will set mixing associated with shallow convection to extend across the inversion only when Equation (1) is satisfied. There are other more sophisticated versions of Equation (1) for CTEI, which quantitatively take into account the "wetness" of the inversion layer (e.g., Nicholls and Turton 1987; Lilly 2002). In our approach, κ can be interpreted as a physically based large-scale tunable-parameter in controlling low-level clouds in a model that is not designed to resolve the detailed structure of low clouds topped boundary layers,

like the GFS. The effectiveness of our criterion will be validated "a posteriori" by the results obtained by the CFS with our revisions.

The GFS also includes a background eddy vertical diffusion to enhance mixing close to the surface, where eddy diffusion calculated by the boundary layer parameterization is considered inadequate. The coefficient of background diffusion decreases exponentially with pressure, with surface value set to 1.0 m^2s^{-1}. For the SEP region, particularly near the coast of South America, the inversion height usually is very low due to strong subsidence. The background vertical diffusion is strong enough to weaken the inversion and allow moisture exchanges with the free atmosphere. Since we have defined inversion height we can now set the background diffusion to zero in layers above the inversion.

4. Description of the experiments

We performed in total four sets of GFS experiments as listed in Table 1. In these experiments, we used a T126 version of the model and version 2 of the Relaxed Arakawa-Schubert (Moorthi and Suarez 1992, 1999) parameterization for the deep convection scheme. Observed SST was prescribed in the boundary conditions in all four experiments. Simulations started at 00 UTC June 13th and ended at 00 UTC August 5th, 2008. Monthly means in July are used in this study. Analyses are mainly focused in the region of Equator-40S, 110W-70W, which we will refer to as the SEP in the remainder of this paper.

i. The CONTROL experiment was done with the operational treatment of shallow convection and background diffusion.

ii. Experiment CTEI is the same as the CONTROL, except that the definition of the inversion and the criterion for instability expressed by Equation 1 are incorporated.

iii. Experiment ZEROBD sets the background diffusion to 0 in layers above the inversion layer.

iv. Experiment CZ has both the CTEI and the ZEROBD modifications.

Table 1: List of experiments performed in this study

	CTEI condition	ZEROBD condition
CONTROL	No	No
CTEI	Yes	No
ZEROBD	No	Yes
CZ	Yes	Yes

5. Results

a. Cloud cover and cloud water

Figure 1 shows the July mean total cloud cover in the SEP region for the four experiments, and Figure 2 displays an observed climatology corresponding to the International Satellite Cloud Climatology Project (ISCCP) climatology averaged between 1985-1993. There is too little cloudiness in CONTROL and the two experiments in which a single condition is applied (ZEROBD and CTEI). CONTROL produces the least total cloud amount. CTEI obtains more low clouds than ZEROBD. In this experiment, however, cloud generation is important near the coastline where inversion heights tend to be low. CZ produces the best total cloudiness compared with the ISCCP observation. Furthermore, CZ values for total clouds in the region between 5S and 30S are much higher than the combination (maximum) of ZEROBD and CTEI (Figure 3). Section 6 discusses the reasons for this feature.

Figure 4 shows the July mean low-cloud cover in all four experiments, while Figure 5 presents an observed climatology from ISCCP. CONTROL produced too few low clouds, the least among the four experiments. The CTEI condition is more effective than the ZEROBD condition in producing low clouds. The CZ experiment generates the highest low-cloud amounts in the four experiments. In fact, there is too much low cloudiness in CZ compared with ISCCP climatology. Since the total cloud cover in CZ
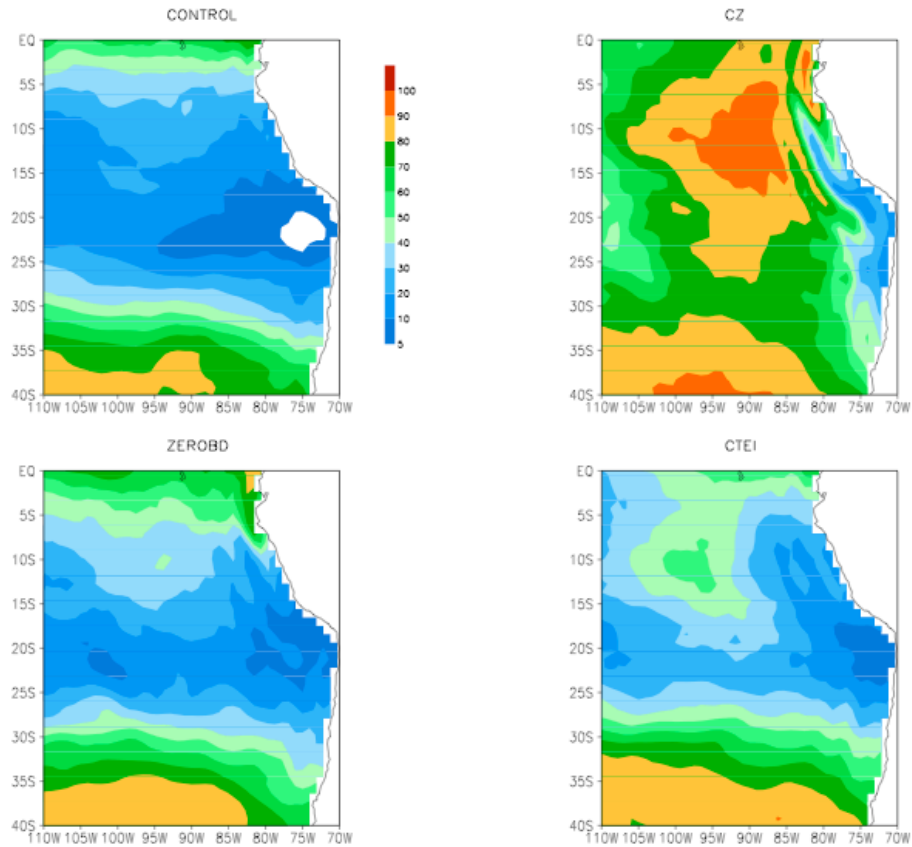
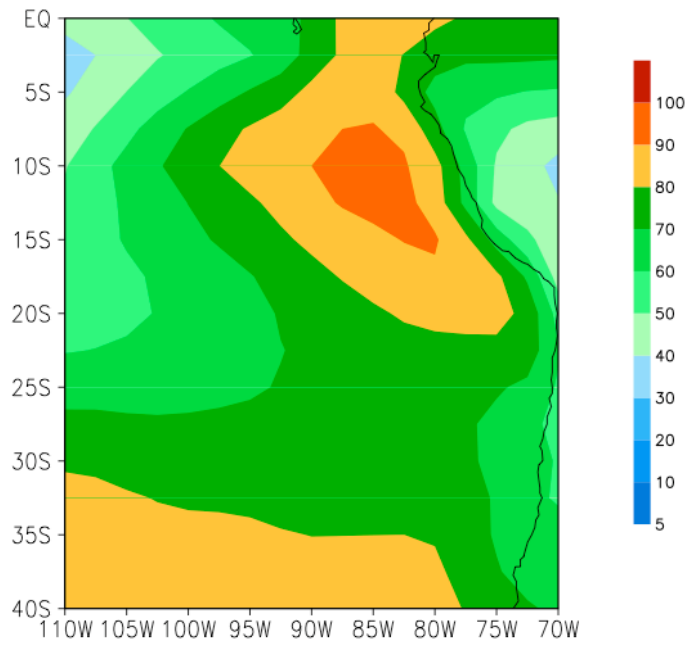Figure 1. The July 2008 mean total cloud cover in the SEP region in all four experiments.

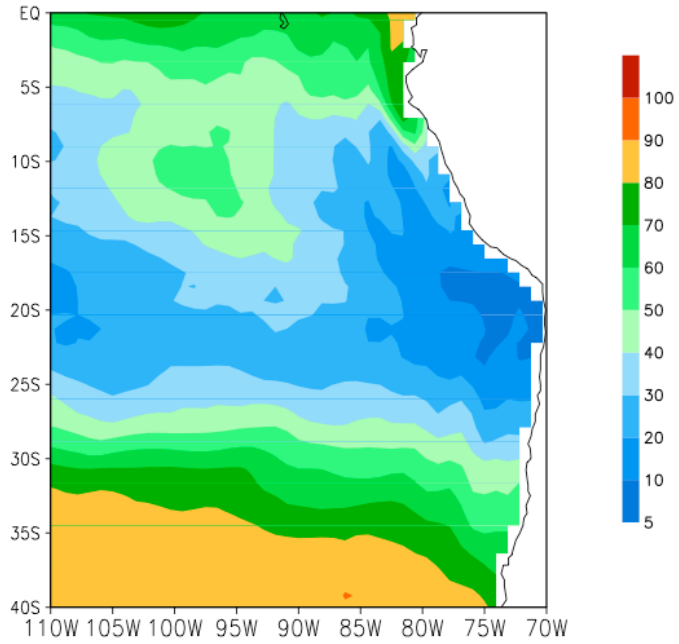Figure 2. The ISCCP July mean (1985-1993) total cloudiness in July in the SEP region

Figure 3. The combined monthly mean total clouds from ZEROBD and CTEI in
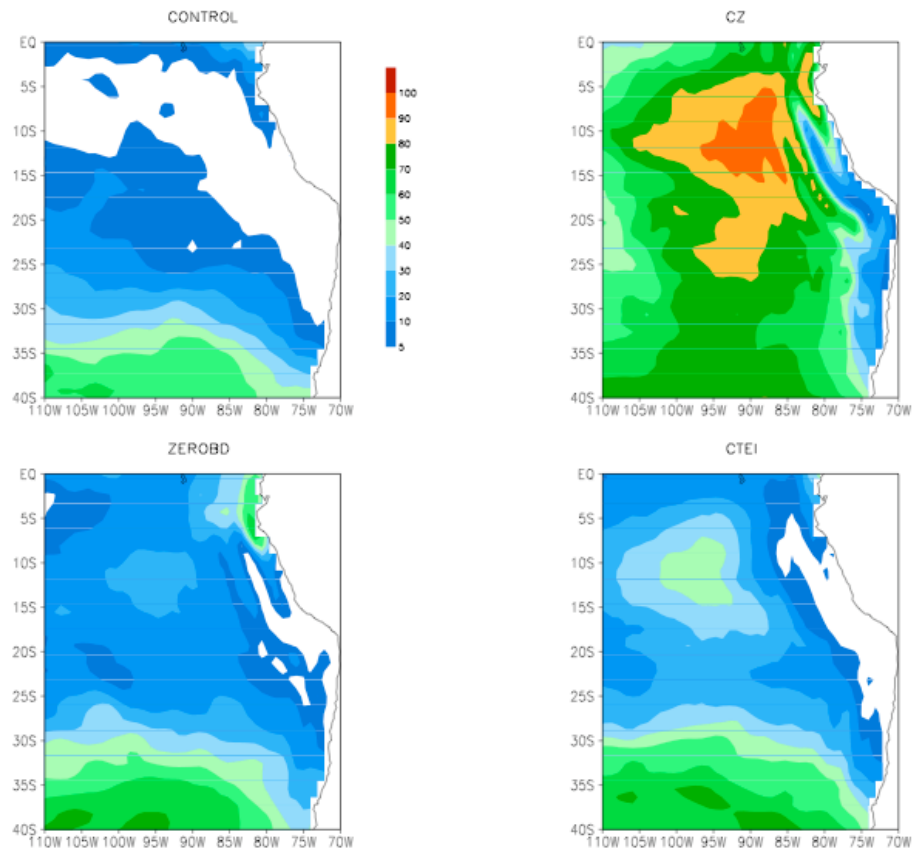July 2008 in the SEP region (not a necessary figure)

Figure 4. As in Fig. 1 except for low clouds

11

is about the same as in the ISCCP climatology, this result suggests a mismatch between the simulated cloud types in CZ and those in the ISCCP climatology. There may be many reasons for this mismatch. One obvious reason is the different low cloud definitions in the GFS and in ISCCP. Clouds from 1000 mb to 680 mb are considered low clouds in ISCCP, while in the GFS low clouds are below 642 mb. Another reason is that ISCCP tends to underestimate low-cloud cover (Chang and Li, 2005; Comments also made by Dr. Chris Fairall at the Second VOCAL meeting in Seattle, 2009). A comparison between Figure 1 and Figure 4 shows that the most of the total clouds in CZ are from low clouds.

Figure 6 shows examples of the vertical structures of cloud water in SEP along 20S. Most of the cloud water produced in the CONTROL is located off the coast. Both the CTEI and ZEROBD experiments generated more cloud water near the coast and at low levels than the CONTROL. The CZ experiment generated the most cloud water, especially at lower levels, much more than the combined amount from both the CTEI and ZEROBD experiments. This is consistent with the fact that vertical diffusion processes in the CONTROL experiment are strong, while CZ allows for mixing across the inversion only when CTEI exists.

b.   *Radiation*

Radiative fluxes at the surface and the top of the atmosphere in the simulations are examined and compared with the corresponding flux climatology averaged between 1984-1994 compiled by the Surface Radiation Budget (SRB) project (http://GEWEX-SRB.larc.nasa.gov/). Since data on cloud amount from ISCCP were used to build the SRB dataset, some degree of consistency between the two datasets are expected. Figure 7 shows the 2008 July mean short-wave radiative flux errors at the surface defined as the differences between the simulated values in the four experiments and the observed climatology from SRB. The short-wave radiative flux at the surface is mostly larger in the CONTROL, ZEROBD, and CTEI experiments than the observed value in SRB, consistent with less cloudiness than the observed climatology in ISCCP. The short-wave
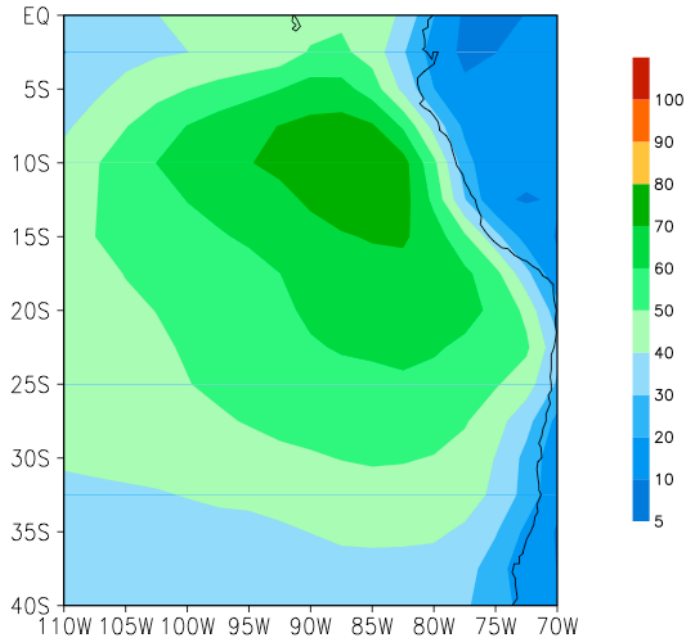
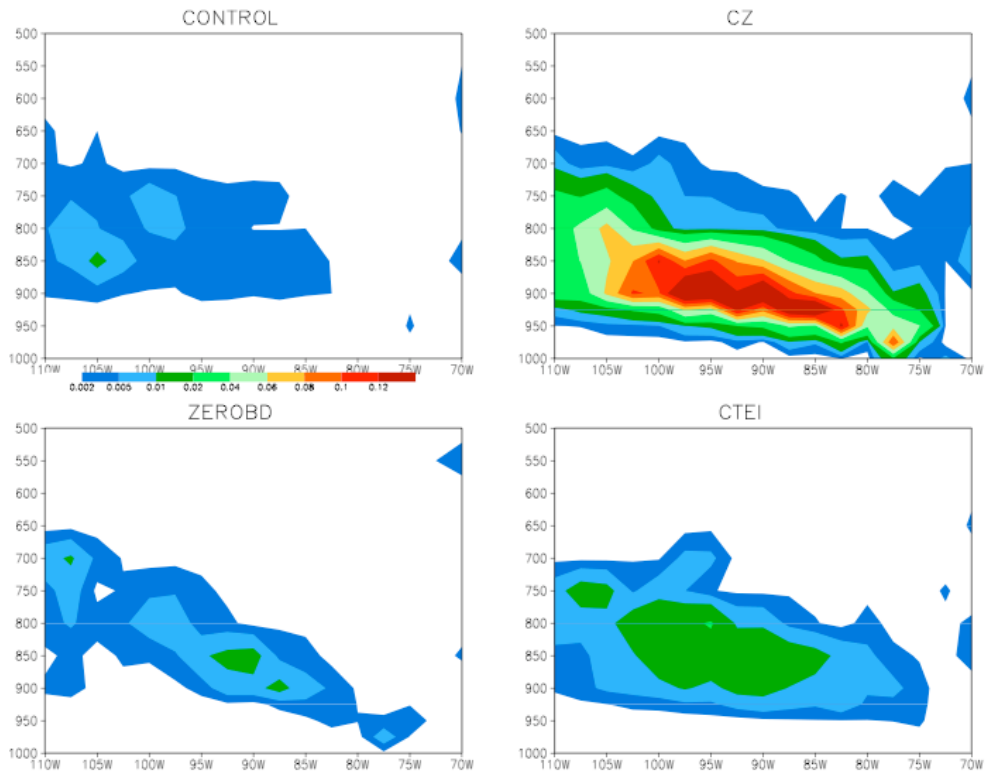Figure 5. As in Fig 2 except for low clouds

Figure 6. Vertical cross-section of monthly mean cloud water in July along 20S.

radiative flux at the surface in CZ is smaller than that in SRB in most of the VOCALS region (except for the portion near the coast) due to more clouds generated in the simulation than the climatology. It should be pointed out that either tuning the microphysics, the shortwave parameterization, or the CTEI tunable parameter could alleviate the excessive absorption of shortwave. It is a known fact that the shortwave parameterization used in this version of GFS absorbs too much shortwave radiation (Y. Hou, personal communication). In terms of the downward long-wave radiative flux at the surface, CZ is much better than the other three simulations shown in Figure 8. The difference in long-wave radiative flux at the surface between CZ and the SRB climatology is small, except near the coastal region. In the other 3 simulations, the long-wave radiative fluxes at the surface are mostly smaller than the climatology due to the shortage of low clouds. Figure 9 shows the July 2008 mean upward radiative flux errors at the top of the atmosphere (TOA). The radiative fluxes at the TOA also reflect the cloudiness generated in the simulations. More upward short-wave radiative flux is produced at the TOA in CZ than in the other three simulations because the latter produces more cloudiness. Compared with the SRB climatology, the upward short-wave radiative flux away from the coast at the TOA is too large in CZ and too small in the other three simulations. The outgoing long wave radiation (OLR) errors at the TOA are illustrated in Figure 10. Values of OLR are large in all simulations compared with the observations. The differences in OLR between CZ and the SRB climatology are smallest.

c.   Surface winds and latent heat flux

Figure 11 shows surface winds in the four experiments. From the equator southward, all experiments show the transition between low-latitude trades and mid-latitude westerlies. A striking difference among the four experiments is the strength of the trade winds. Trade winds in the ZEROBD and in the CZ experiments especially near the coast are stronger than in the CONTROL, while the trade winds are smaller in the CTEI. The width of the transition region and the strength of the westerlies are also very different
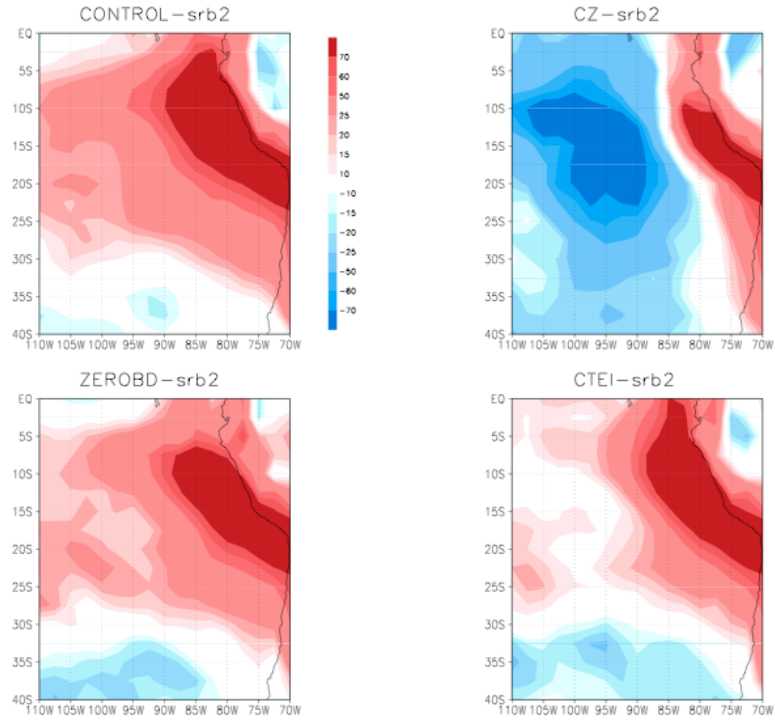
Figure 7. The July 2008 mean surface downward shortwave radiative flux errors
(difference between the four simulations and SRB climatology)
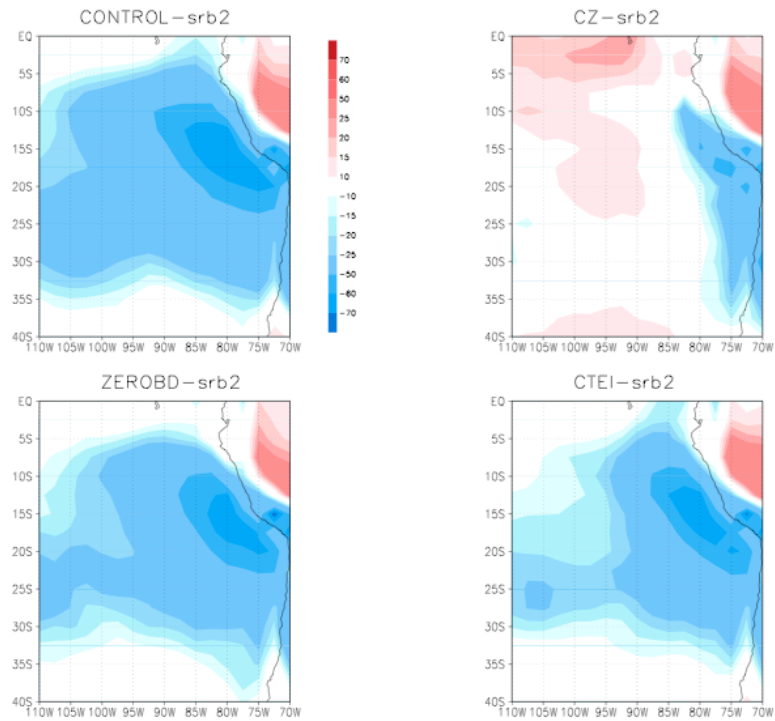

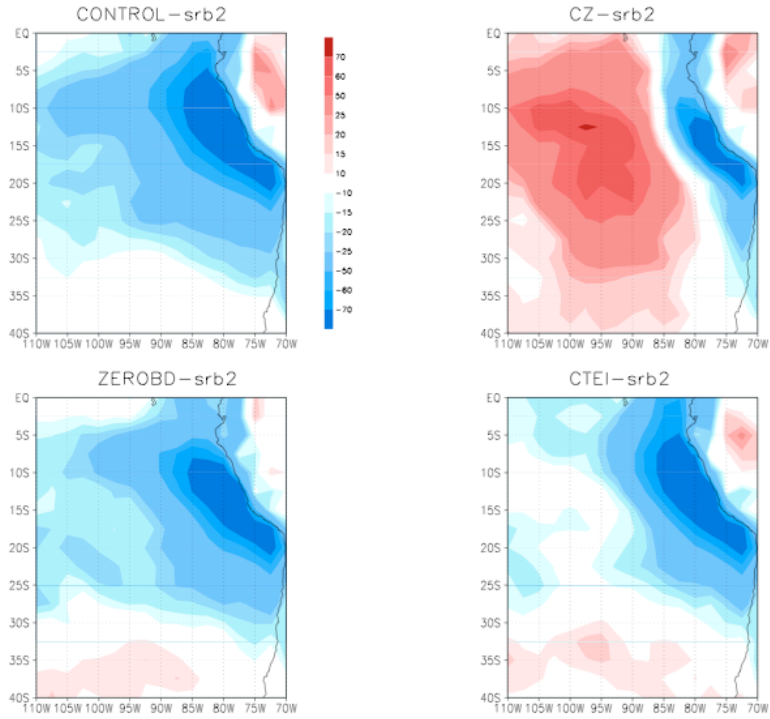Figure 8. As in Fig. 7 except for longwave radiative flux errors

Figure 9. The July 2008 mean upward shortwave radiative flux errors (difference between the simulations and SRB climatology) at the top of the atmosphere in the four experiments.
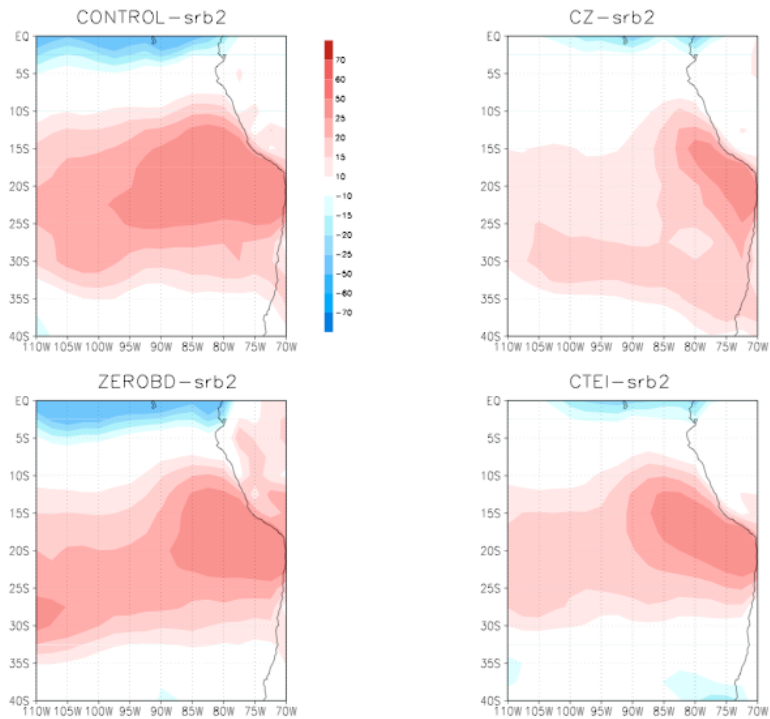

Figure 10. As in Fig.9 except for the longwave radiative flux errors

among the experiments. The transition regions are larger and westerlies are weaker in CZ and CTEI than in CONTROL and ZEROBD. The transition region is smallest and westerlies are strongest in ZEROBD while the opposite is true for CTEI. Figure 12 shows the latent heat fluxes in the four experiments. To some degree the latent heat fluxes reflect the wind intensity. For instance, in the trade wind region, the latent heat flux is largest in CZ corresponding to the strongest winds. However, wind alone does not determine the latent heat flux. The latent heat fluxes are smaller in CZ between 35 S and 40 S than that in CTEI despite the stronger winds in CZ, which indicates that the moisture difference between the sea surface and the air above is smaller in CZ than in CTEI.
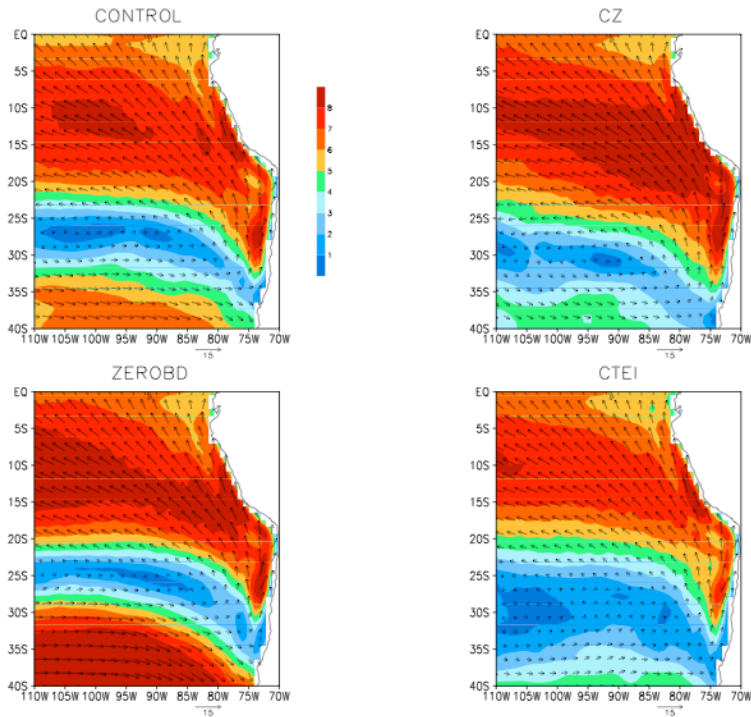

Figure 11. The July 2008 mean surface wind magnitude (shaded ms^{-1}) and direction (arrows) in the four experiments.
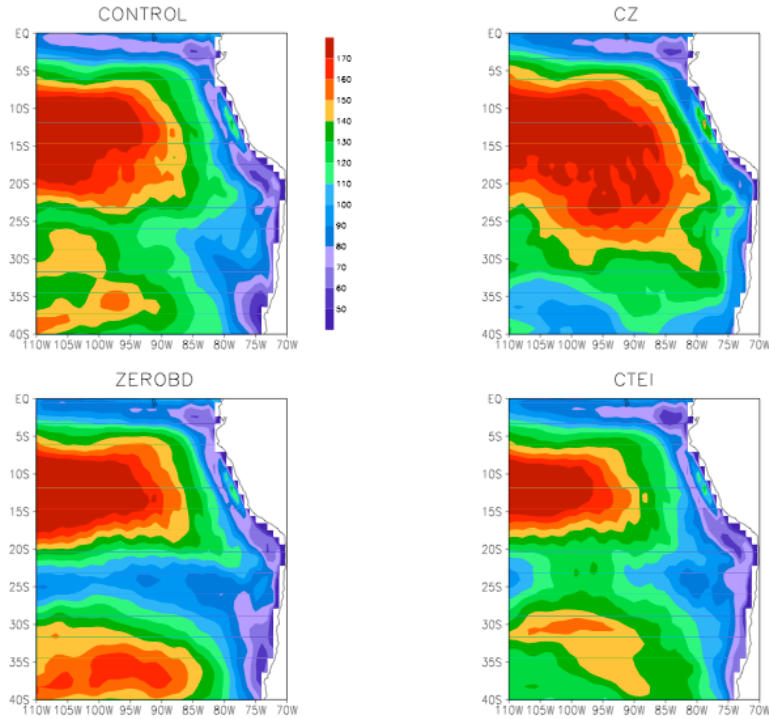
Figure 12. The July 2008 mean surface latent heat flux (W m^2) in the four experiments

6. Relative impact of ZEROBD and CTEI conditions

The shallow convection scheme in the GFS acts through enhanced diffusion in the cloudy layers. The scheme warms and dries the lower layers and cools and moistens the upper layers. Figure 13 shows vertical cross-sections of monthly mean moistening rates along 20S from 110W to 70W due to shallow convection in the four experiments. Mixing is the most intense in CONTROL and the least intense in CZ. Mixing in CTEI is weaker than that in ZEROBD. The mixing layers in CONTROL and ZEROBD are thicker than in CTEI and CZ. We surmise that the lower amount of mixing in CZ is the main reason for the greater cloudiness in the experiment. Due to less mixing, more moisture is trapped at low levels in CZ than in the other three experiments. Then, the large-scale condensation (microphysical process) and, to a certain extent, RAS, take over to produce more clouds. The ZEROBD experiment does not directly reduce mixing due to shallow convection. But, by reducing background mixing, it tends to increase the strength of the inversion, which then reduces the chance of shallow convection activity by decreasing convective available potential energy (CAPE). When combined with CTEI in CZ, this increase in the

18

strength of the inversion due to ZEROBD probably has an additional impact. With a stronger inversion, the CTEI condition tends to allow less shallow convection activity according to Eq. (1). Figure 14 shows the monthly mean vertical cross-sections of heating rate (shaded) due to large-scale condensation/evaporation and temperature (contours) along 20S in the four experiments. Positive heating rate (warming) due to large-scale condensation is only found in CZ. Negative heating rates (cooling) in the other three experiments and at low levels in CZ are due to the evaporation of cloud and rainwater. The most intense warming in CZ happened roughly below the inversion (inversion height changes with longitude and with time), which is where most clouds are produced. The RAS also produces clouds through detrainment of cloud water at the cloud top. Figure 15 illustrates the convective heating rate due to RAS, where the RAS is most active in CZ and is more active in CTEI than in CONTROL or ZEROBD. Since large-scale condensation did not help to produce clouds in CONTROL, ZEROBD, and CTEI, it was RAS that produced clouds through detrainment in these experiments. Clouds in CZ are generated both through RAS and in-situ large-scale condensation. Reduced moisture diffusion under the inversion allows for increased relative humidity leading to large-scale condensation below inversion. The RAS also provides more moisture near the inversion through detrainment, which results in large-scale condensation. However, large-scale condensation is the main process producing the clouds. Figure 16 illustrates the vertical cross-sections of heating rates due to large-scale condensation overlaid with cloud water mixing ratios. In Figure 16 the most dramatic heating rates occur in the region of the most cloud water. Besides producing clouds by detraining cloud water at the cloud top, RAS also indirectly contributes to the cloud production in CZ by reducing mixing by shallow convection. This is because shallow convection is shut off whenever RAS is activated unless the cloud depth is less than 200 hPa.

7. Impacts on global precipitation

Figure 17 shows the July 2008 mean global precipitation rate (mm/day) in the four experiments. The Climate Prediction Center (CPC) Merged Analysis of Precipitation (CMAP; Xie and Arkin, 1996) climatology averaged between 1979-2005 is shown in Figure 18. Compared with CONTROL, the other three experiments produce more
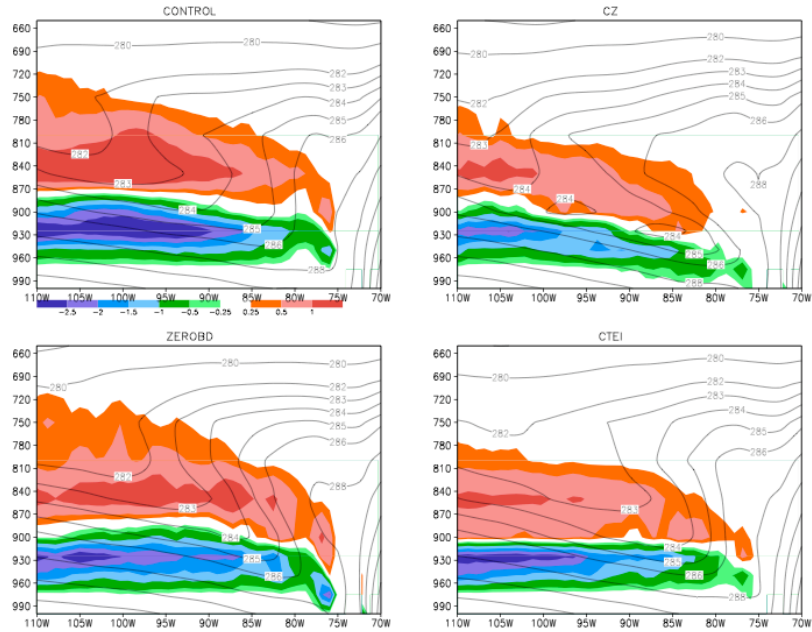
Figure 13. Vertical cross-sections of monthly mean moistening rates (g/kg/day) along 20S in shades due to shallow convection in the four experiments. Contours represent vertical cross-section of temperature.
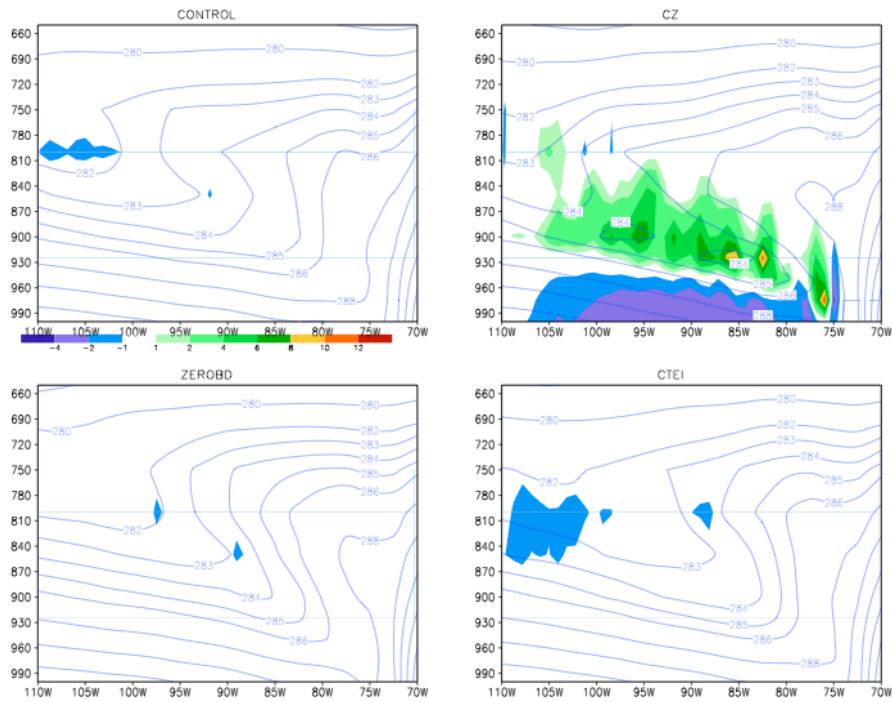

Figure 14. As in Fig. 13 except for the heating rate (K/day) (shaded) due to large-scale condensation.
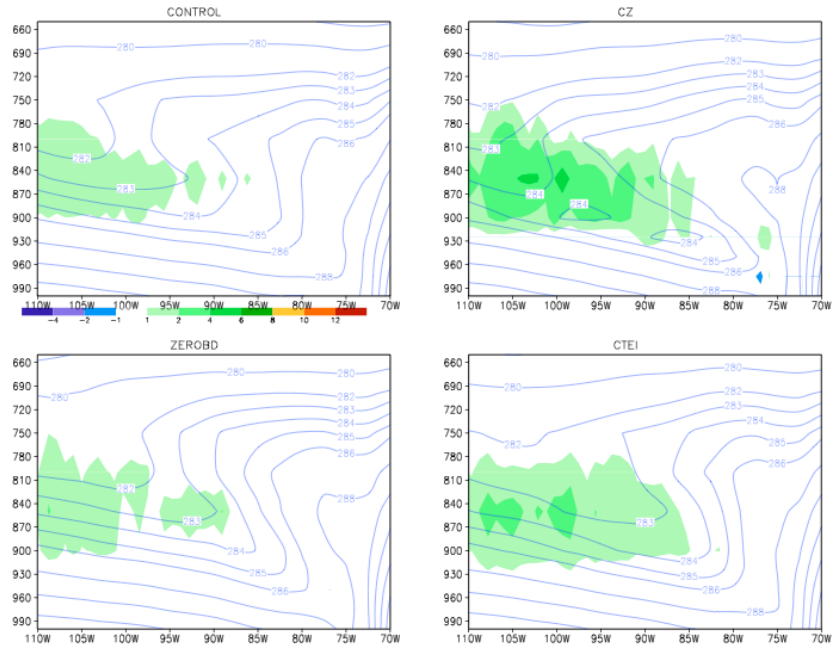
Figure 15. As in Fig. 13 except for convective heating rate (K/day) due to RAS
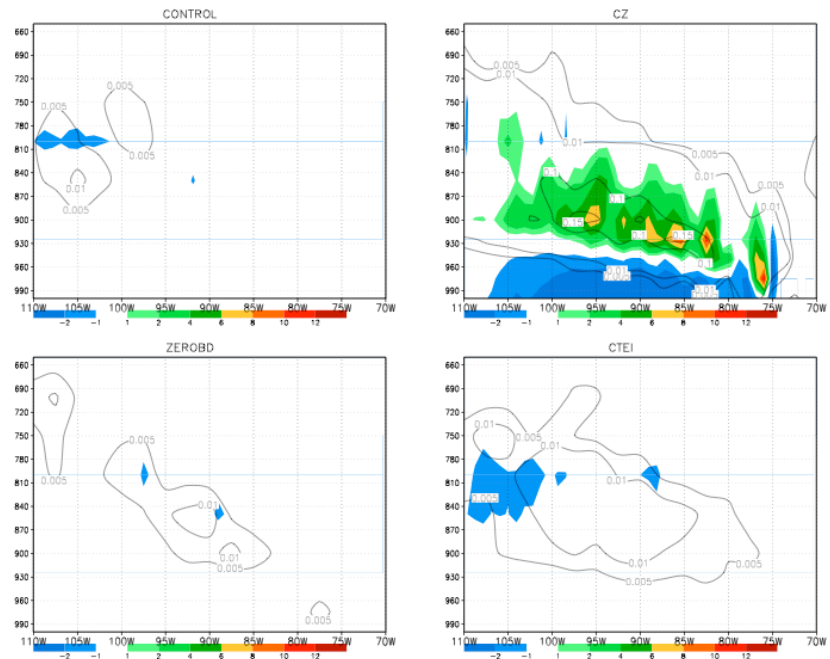

Figure 16. Vertical cross-sections of monthly mean heating rate due to large-scale condensation (K/day) along 20S in shades overlaid with monthly mean cloud water mixing ratios (g/kg) in contours

21

precipitation over the western Pacific warm pool and maritime continental area and less precipitation over the eastern Pacific ITCZ. The CZ produces the most precipitation in the west Pacific and least in the east Pacific among all four experiments. The precipitation rate is smaller in the southern pacific convergence zone (SPCZ) and larger in the mid-Pacific ITCZ in CZ than in the CONTROL. An interesting feature that occurs only in CZ is the 1-2 mm/day precipitation rate in the SEP region. This light precipitation is primarily caused by large-scale processes. In reality, this is the region where drizzle occurs. Compared with the CMAP climatology most of the main precipitation features are produced in the four experiments, for instance, rain bands associated with the ITCZ, SPCZ, the mid-latitude oceanic storm tracks, and the tropical continental maxima. The precipitation intensities in these regions from the experiments differ from CMAP in that too much precipitation is produced over the western warm pool and the east tropical Pacific. The ITCZ in the four experiments are narrower than in CMAP. Since precipitation in the simulations are only one-month means and the CMAP precipitation is monthly means averaged over many years, the differences in precipitation intensity and the width of the ITCZ between the simulations and CMAP may not be surprising.

8. Summary

Several methods have been tested in the NCEP GFS model to alleviate an important systematic error: the lack of stratocumulus in the SEP region. This paper described two simple modifications: (a) elimination of background vertical diffusion above the low-level inversion (ZEROBD), and (b) incorporation of a tunable parameter based on the CTEI criterion for determining cloud tops for the shallow convection parameterization when low-level inversions exist (CTEI). Four simulations were performed to examine the individual effect of each modification and the combined effect of the two modifications on the generation of the stratocumulus clouds. Both modifications enhanced clouds generation in the SEP region. The CTEI is more effective than ZEROBD in producing low-level clouds. However, ZEROBD is also shown to be important, especially close to the coast. A comparison with the ISCCP climatology reveals that both modifications individually produced too little cloudiness. However, the

two modifications applied together produced about the right amount of total cloudiness in the region. The combination is much more effective than any of the two modifications alone. The reason for this nonlinearity is that both changes reinforce each other in reducing the leakage of moisture across the inversion. Less mixing traps more moisture in lower levels below the inversion and results in more condensation. This enhanced response in the combined case also implies that the effectiveness of the CTEI-based algorithm depends sensitively on the strength of the inversion. In generating clouds the large-scale condensation process was the main contributor. The RAS scheme also provided a positive, but small contribution. Although roughly of the correct magnitude, the amount of total cloudiness obtained in the simulation with both modifications may produce different low, middle, and high cloud amounts than the observations. The availability of reliable observations of the vertical distribution of cloud water will be very helpful for verifying climate models. The impacts of this mismatch on the coupled climate system simulation have yet to be studied.
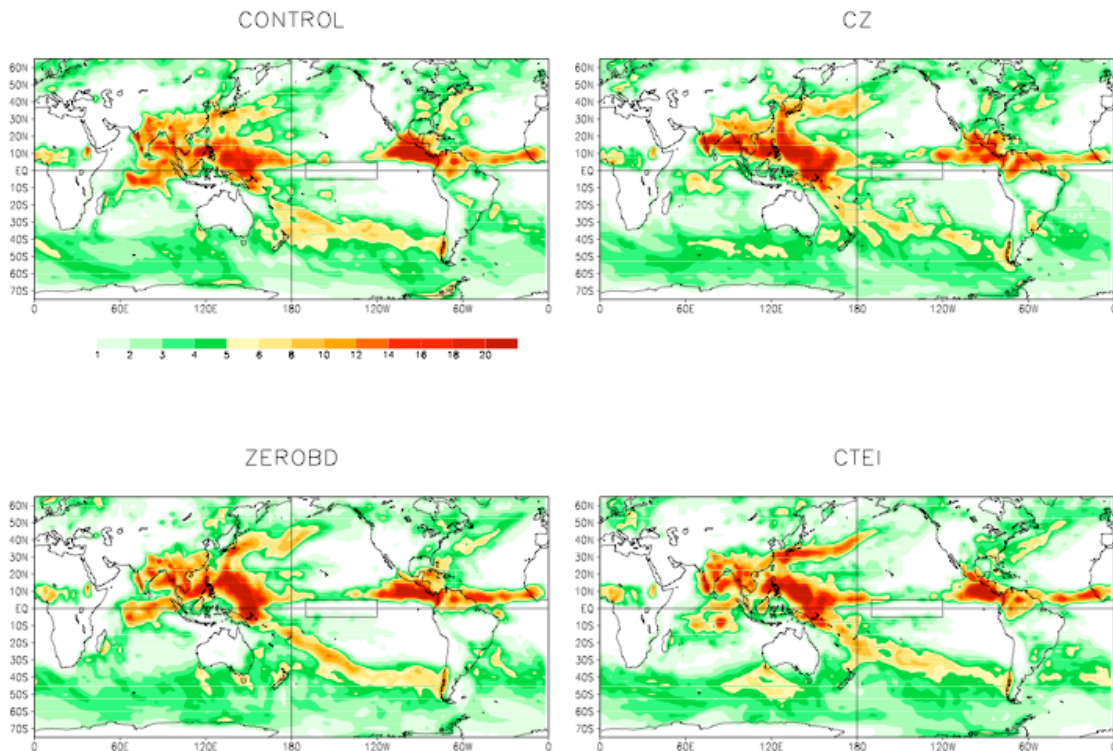

Figure 17 The July 2008 mean precipitation rate (mm / day) in the four experiments.
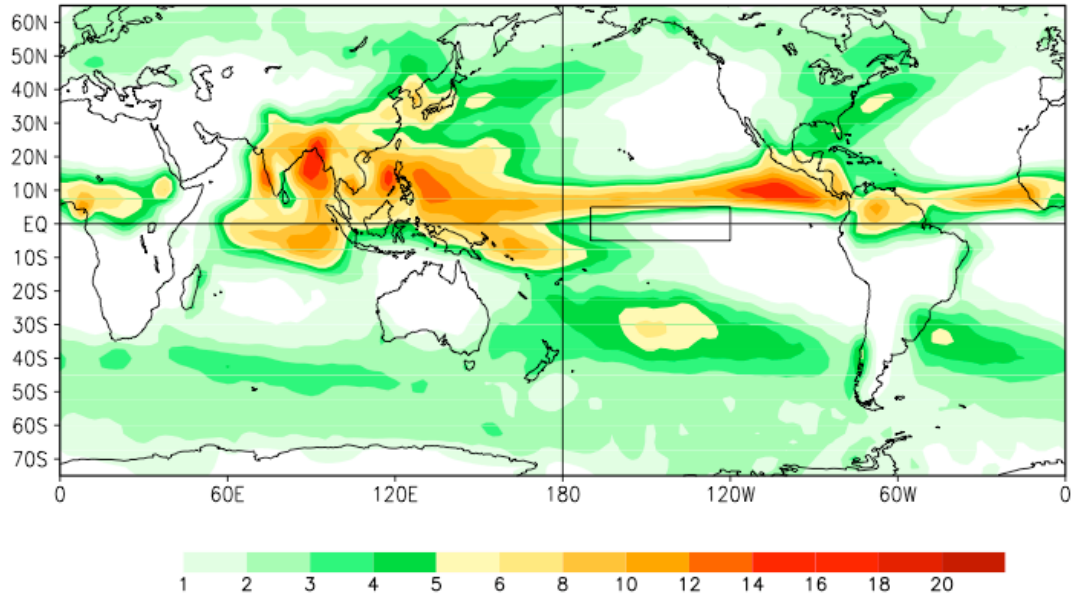
Figure 18. The global July mean CMAP precipitation rate (mm/day) averaged between 1979 and 2005 (Xie and Arkin, 1997)

Our experiments have demonstrated that it is possible to simulate realistic marine boundary clouds in large-scale models with relatively simple and physically based changes in the major model parameterizations. Although the CZ experiment may have produced too much cloud cover or too much cloud water, it is possible to further improve these fields by slightly modifying the microphysics, and/or cloudiness parameterizations, and/or the CTEI tunable parameter. This should also reduce the excessive reduction of shortwave radiation at the ocean surface. NCEP is currently moving towards implementing in its operational models the RRTM shortwave radiation parameterization with maximum/random overlap. This radiation scheme has less shortwave absorption in the clouds, which together with a slightly tuned microphysics should further improve the surface shortwave radiation at the ocean surface. At the present time, the two modifications presented in this paper have been implemented in the model in the new CFS reanalysis (Saha et al., 2010).

generous help with the GFS/CFS. We appreciate helpful comments from Drs. Brad Ferrier and Glenn White during the internal review process.

REFERENCES

Alpert, J.C., 2004: subgrid-scale mountain blocking at NCEP. Proc. *Of 20th conf. on Weather and Forecasting*, Seatle, WA.

Bony, S. and J.-L.Dufresre, 2005: Marine boundary layer clouds at the heart of tropical cloud feedback uncertainties in climate models, *Geopys. Res. Lett.,* **32**, L20806, doi:10.1029/2005GL023851

Chang, F. and Z. Li, 2005: A near-global climatology of single-layer and overlapped clouds and their optical properties retrieved from Terra/MODIS data using a new algorithm, *J. Climate*, **18**, 4752-4771

Chou, M.D, M. J. Suarez, C. H. Ho, M. M. H. Yan, and K. T. Lee, 1998: Parameterizations of cloud overlapping and shortwave single scattering properties for use in general circulation and cloud ensemble models. *J. Climate*, **11**, 202-214

Deardorff, J.W., 1980: cloud top entrainment instability, *J. Atmos. Sci.*, **37**, 131-147

Hannay, C., D.L. Williamson, J.J. Hack, J.T. Kiehl, J.G. Olson, S.A. Klein, C.S. Bretherton, and M. Köhler, 2009: Evaluation of Forecasted Southeast Pacific Stratocumulus in the NCAR, GFDL, and ECMWF Models. *J. Climate*, **22**, 2871–2889.

de Szoeke, S.P., Y. Wang, S.-P. Xie, and T. Miyama, 2006: Effect of shallow cumulus convection on the eastern Pacific climate in a coupled model. *Geophys. Res. Lett.,* 33, L17713, doi:10.1029/2006GL026715

Ek M.B., K.E. Mitchell, Y. Lin, E. Rogers, P. Grummann, V. Koren, G. Gayno, and J.D. Tarplay, 2003: Implementation of the Noah land-use model advances in the NCEP operational mesoscale Eta model. *J. Geophys. Res.* **108**, 8851, doi:10.1029/2002JD003296

Gordon, C.T., A. Rosati, and R. Gudgel, 2000: Tropical sensitivity of a coupled model to specified ISCCP low clouds. *J. Climate*, **13**, 2239-2260

Hong, S. -Y. and H. -L. Pan, 1996: Nonlocal boundary layer vertical diffusion in a

medium range forecast model. *Mon. Wea. Rev.,* **124**, 2322-2339.

Hong, S. -Y. and H. -L. Pan, 1998: Convective Trigger Function for a Mass-Flux Cumulus Parameterization Scheme. *Mon. Wea. Rev.*, **126**, 2599–2620.

Hou, Y. -T., K. A. Campana and S.–K. Yang, 1996: Shortwave radiation calculations in the NCEP's global model. *Int. Radiation Symposium*, IRS-96, August 19-24, Fairbanks, AL.

Hou, Y., S. Moorthi, and K. Campana, 2002: Parameterization of solar radiation transfer in the NCEP models. *NCEP Office Note*, 441.

http://www.emc.ncep.noaa.gov/officenotes/FullTOC.html#2000.

Kalnay, E. and Coauthors, 1996: The NCEP/NCAR 40-year Reanalysis Project. *Bull. Amer. Meteor. Soc.,* **77**, 1057-1072.

Klein, S.A., and D.L. Hartmann, 1993: The seasonal cycle of low stratiform clouds. *J. Climate,* **6**, 1587-1606.

Kollias, P., C.W. Fairall, P. Zuidema, J. Tomlinson, and G.A. Wick, 2004: Observations of marine stratocumulus in SE Pacific during the PACS 2003 cruise. *Geophs. Res. Lett.*, **31**, L22110

Kuo, H., and W.H. Schubert, 1988: Stability of cloud-topped boundary layers. *Quart. J. Roy. Meteor. Soc.*, **114**, 887–917.

Lock, A.P., 2009: Factors influencing cloud area at the capping inversion for shallow cumulus clouds. *Quart. J. Roy. Meteor. Soc* **135**(641): 941

Lilly, D.K., 2002: Entrainment into mixed layers. Part III: A new closure. *J. Atmos. Sci.*, **59**, 3353-3361

Lott, F. and M. J. Miller, 1997: A new subgrid-scale orographic drag parameterization: Its performance and testing. *Quart. J. Roy. Meteor. Soc.,* 123, 101-127

Ma, C.-C., C.R. Mechoso, A.W. Robertson and A. Arakawa, 1996: Peruvian stratus clouds and the tropical Pacific circulation: A coupled ocean-atmosphere GCM study. *J. Climate*, **9**, 1635-1645.

MacVean, M.K., and P.J. Mason, 1990: Cloud-top entrainment instability through small-

scale mixing and its parmeterization in numerical models. *J. Atmos. Sci.*, **47**, 1012-1030

Mechoso, C.R., and coauthors, 1995: The seasonal cycle over the tropical Pacific in coupled ocean-atmosphere general circulation models. *Mon. Wea. Rev.*, **123**, 2825-283

Mechoso, C.R. and coauthors, 2005: VAMOS Ocean-Cloud Atmosphere-Land Study (VOCALS) Science Paln, 42 PP. [Available online at http:www.eol.ucar.edu/projects/vocals/science_planning/VOCALS-Science-Plan.pdf]

Mlawer E. J., S. J. Taubman, P. D. Brown, M.J. Iacono and S.A. Clough, 1997: radiative transfer for inhomogeneous atmosphere: RRTM, a validated correlated-K model for the longwave. *J. Geophys. Res.*, 102(D14), 16,663-16,6832.

Moeng C.-H., 2000: Entrainment rate, cloud fraction and liquid water path of PBL stratocumulus clouds. *J. Atmos. Sci.,* **57**, 3627–3643

Moorthi, S., and M. J. Suarez, 1992: Relaxed Arakawa-Schubert. A Parameterization of Moist Convection for General Circulation Models. *Mon. Wea. Rev.*, **120**, 978- 1002.

Moorthi, S., and M. J. Saurez, 1999: Documentation of version 2 of Relaxed Arakawa-Schubert cumulus parameterization with convective downdrafts. *NOAA Tech. Report* NWS/NCEP 99-01, 44pp

Moorthi, S., H. L. Pan and P. Caplan, 2001: Changes to the 2001 NCEP operational MRF/AVN global analysis/forecast system. *NWS Technical Procedures Bulletin*, 484, pp14. [Available at http://www.nws.noaa.gov/om/tpb/484.htm]

Nicholls S.k and J.D. Turton, 1986: an observational study of the stracture of stratiform cloud streets. Art II: Entrainment. *Quart. J. Roy. Meteor. Soc.*, **112**, 461-480

Pan, H.-L. and W.-S. Wu, 1995: implementing a mass flux convective parameterization package for the NMC medium range forecast model. *NMC office note* 409, 40 PP.[Available online at http://www.emc.ncep.noaa.gov/officenotes/FullTOC.html#1990]

Randall, D. A., 1980: conditional instability of the first kind upside-down. *J. Atmos. Sci*, **37**, 125-130

Saha, S. and Coauthors, 2006: The NCEP climate forecast system, *J. Climate*, **19**, 3483-3517

Saha, S., and Coauthors, 2010: The NCEP climate forecast system reanalysis. *Submitted to Bull. Amer. Met. Soc.*

Sela, 2009: Implementation of the sigma pressure hybrid coordinate into GFS. *NCEP office Note* # 461[available at http://wwww.emc.ncep.noaa.gov/officenotes/FullTOC.html#2000].

Siems, S.T., C.S. Bretherton, M.B. Baker, S.S. Shy, and R.E. Breidenthal,1990: Buoyancy reversal and cloud-top entrainment instability.Quart. *Quart. J. Roy. Meteor. Soc.,* 116, 705–739.

Stevens, B., C.H. Moeng, A.S. Ackerman, C.S. Bretherton, A. Chlond, S. de Roode, J. Edwards, J.C. Golaz, H. Jiang, M. Khairoutdinov, M.P. Kirkpatrick, D.C. Lewellen, A. Lock, F. Müller, D.E. Stevens, E. Whelan, and P. Zhu, 2005: Evaluation of Large-Eddy Simulations via Observations of Nocturnal Marine Stratocumulus. *Mon. Wea. Rev.*, **133**, 1443–1462.

Sundqvist, H., E. Berge, and J. E. Kristjansson, 1989: Condensation and cloud studies with mesoscale numerical weather prediction model. *Mon. Wea. Rev.,* **117**, 1641-1757.

Tiedtke, M., 1983: The sensitivity of the time-mean large-scale flow to cumulus convection in the ECMWF model. *ECMWF Workshop on Convection in Large-Scale Models,* 28 November – 1 December 1983, Reading, England, pp. 297-316.

Wang, W., S. Saha, H.-L. Pan, S. Nadiga, G. White, 2005: Simulation of ENSO in the new NCEP coupled forecast system model (CFS03), *Mon. Wea. Rev.,* **133**, 1574-1593

Wang, Y., H. Xu, and S.P. Xie, 2004: Regional model simulations of marine boundary layer clouds over the southeast Pacific off South America. Part II: sensitivity experiments. *Mon. Wea. Rev.,***132**, 2650-2668

Xie, P., and P.A. Arkin, 1997: Global precipitation: a 17-year monthly analysis based on gauge observation, satellite estimates, and numerical model outputs. *Mon, Wea. Rev.,* 78, 2539-2558.

Xu, K.M., and D.A. Randall, 1996: A semiemperical cloudiness parameterization for use in climate models. *J. Atmos. Sci.*, 53, 3084-3102

Zhao, Q. Y., and F. H. Carr, 1997: A prognostic cloud scheme for operational NWP models. *Mon. Wea. Rev.,* **125**, 1931-1953.